Scientific Reviews & Chemical Communications

Research Article | Vol 7 Iss 2

Interacting Bose Gas in a Harmonic Trap

Smail Kouidri*

Department of Physics, University of Saida, Algeria

***Corresponding author:** Smail Kouidri, Department of Physics, University of Saida, 20000 Algeria, E-mail: kouidris@yahoo.fr

Received: June 13, 2017; **Accepted:** August 4, 2017; **Published:** August 8, 2017

Abstract

We devote a particular attention to the role played by the repulsive interaction on the chemical potential of condensed atoms, the chemical potential of non-condensed atoms, the anomalous fraction and the heat specific capacity for Bose gas in harmonic trap. First, we point out that the generalized Hartree-Fock Bogoliubov approximations (GHFB) produces a change in the specific temperature via estimation experience, and we discuss these inadequacies. We calculate a behavior of condensate density in Thomas Fermi approximation, where the thermal cloud is not negligible. Finally, we compare our results with various recent numerical estimates and experience.

Keywords: Bose einstein condensation (BEC); Generalized hartree-fock bogoliubov approximations (GHFB); Thomas fermi approximation (TFA)

Introduction

The properties of Bose gases have recently attracted great attention both experimentally and theoretically. These interests, in these systems, are based on the initial experiments on alkali atoms as first step and have been extended to diluted gases such as Rb, Na or Li [1-4].

Since then, the field of ultra-cold atoms gave rise to a multitude of experimental and theoretical methods. On the one hand, the experimenters tried to always try to better understand this strange behavior of the material confining gas by different types of potential traps and changing their shapes and structures. They even succeeded in controlling the interactions between atoms by using Feshbach resonance. The gas initially repellents could become attractive and vice versa. It is an extraordinary advance in atomic physics. In addition, the techniques of cooling have become increasingly ingenious and reach temperatures of the order of nanokelvin, pushing the experiences toward zero absolute.

On the other hand, and with the breakthrough experimental techniques, we have seen the development of theoretical models of increasingly sophisticated. One of the first models with a great success was the Gross-Pitaevskii equation (GP) which describes the behavior of gas at exactly zero temperature. This equation, which is typically a nonlinear Schrodinger equation,

Citation: S Vakalis, A Sotiropoulos , K Moustakas, et al. Assessing the Potential of Particleboard Production from Food Waste: Analysis of the Input Materials. Sci Revs Chem Commun. 2017; 7(2):107.

is able to predict correctly many equilibrium properties of quantumgases. The effects of temperature and correlation between condensed atoms (in the state) and non-condensed atoms (excited) are completely ignored in this approximation. In contrast, it takes account the interactions between condensed atoms and predicted with great success the collective excitations of the condensate at zero temperature.

However, if you not taking into account the thermal cloud, it still remained fairly low conceptually. Many generalizations have been proposed [5,33] from Popov approximation, which involves explicitly non-condensed density to that of Beliaev where we see it clear for the first time of many body effects via the anomalous average, itself directly connected to the self-energy and therefore the T matrix scattering.

So in this paper, we use the approximations described above but at finite temperature because they are responsible in determination of general properties of trapped ultra-cold atoms, in particular the chemical potential, energy spectrum and heat capacity as function of temperature and number of particles respectively. In this context and based of the Gross-Pitaevskii equation which gives the proper state of system exactly, we can discuss various state. The interactions between atoms are responsible to describe the different properties. We note here, that we take in account the Yukalov rules [34] in determination of the chemical potential. We inject this rule in our numerical algorithm [35] we are able to find this quantity.

The paper is organized as follows. In Sec-II we set up the formalism needed to treat an interacting Bose gases within the generalized Hartree-Fock Bogoliubov approximation (GHFB). We analyze, in Sec-III results and discussion, the influence of the trap potential and the interactions on the chemical potential of the gas. We show that the interactions have important effects on the chemical potential. We investigate the behavior of the heat capacity. We find that at sufficiently low temperatures the interactions change the qualitative behavior of the heat capacity. This is explained in terms of the effects the interactions have on the quasi particle spectrum. Finally, we summarize the results in Sec-IV.

Formalism

We will consider a spherically symmetric harmonic trap, the condensate wave function, φ_0 (r), may be chosen real [5] and may be verify the Gross-Pitaevskii equation, which is simply the Euler Lagrange of the energy functional of the dilute Bose gases. It reads:

$$\left(\frac{-\hbar^2}{2m}\Delta + V_{trap}(r) + g[n_c(r) + 2\tilde{n}(r) + \tilde{m}(r)] \right)\varphi_0(r) = \mu\varphi_0(r) \qquad (1)$$

Where:

$V_{trap}(r) = \frac{1}{2}\omega^2 r^2$ is the trap potential, $g = \frac{4\pi\hbar^2 a}{m}$ is the strength interaction, and $n_c(r), \tilde{n}(r), \tilde{m}(r)$ are the condensate density, the non-condensate density and the anomalous density respectively. To simplify the notation, the energies will be measured in units of, $\hbar\omega$ is determined by the quasi particles amplitudes $\left(u_i(r), v_i(r)\right)$ and quasiparticles energies, E_i, which obey the coupled Bogoliubov-de Gennes (BdG) equations:

$$Lu_i(r) - g(n_c(r) + \tilde{m}(r))v_i(r) = E_i u_i(r) \quad (2)$$

$$Lv_i(r) - g(n_c(r) + \tilde{m}(r))u_i(r) = -E_i v_i(r) \quad (3)$$

Here:

$$L = \frac{-\hbar^2}{2m}\Delta + V_{trap}(r) - \mu + 2g(n_c(r) + \tilde{n}(r))$$

By expanding the quasiparticles amplitudes, $(u_i(r), v_i(r))$ via a spherical harmonics basis:

$$(u_i(r), v_i(r)) = \sum_{l=0}^{\infty} \sum_{m=-1}^{l} \frac{(u_i(r), v_i(r))}{r} Y_{lm}(r) \quad (4)$$

We can determine the analytic form of the condensate, the non-condensate and the anomalous density:

$$N_c \mid \varphi_0 \mid^2 = n_c(r) \quad (5)$$

$$\tilde{n}(r) = \sum_{l=0}^{l_{\max}} \frac{2l+1}{4\pi r^2} \sum_{n_l=0}^{n_{l\max}} \left(|u_{l_{n_l}}(r)|^2 + |v_{l_{n_l}}(r)|^2 \right) f_B\left(E_{l_{n_l}}\right) + \mid v_{l_{n_l}}(r) \mid^2 \quad (6)$$

$$\tilde{m}(r) = \sum_{l=0}^{l_{\max}} \frac{2l+1}{4\pi r^2} \sum_{n_l=0}^{n_{l\max}} u^*_{l_{n_l}}(r) v_{l_{n_l}}(r) \left(1 + 2 f_B\left(E_{l_{n_l}}\right)\right) \quad (7)$$

$f_B\left(E_{l_{n_l}}\right)$ is the Bose-Einstein function :

$$z^{-1} = 1 + N_c^{-1} \quad (9)$$

With fugacity z^{-1}

$$z^{-1} = 1 + N_c^{-1} \quad (9)$$

$\beta = \frac{1}{k_B T}$ is the inverse temperature. The chemical potential is determined, by using the Yukalov rule [34].

The equations (1-3) form a closed set to be solved self-consistently. We have chosen in our numerical calculations the couple (n; l) up to (n_{max}, l_{max}) beyond which values the results of the coupled equations (1-3) remain unchanged.

Results and Discussions

Let us consider a ^{87}Rb gas $(m = 1.44 \times 10^{-25}\, Kg)$ with s-wave scattering length $a = 5.82 \times 10^{-9}\, m$ in a harmonic trap with frequency $\omega = 2\pi \times 200\, Hz$. We started by calculating the chemical potential.

The chemical potential

In this section we will determine the chemical potential μ as a function of the temperature and number of particles in the trap. Yukalov [34] has done an extensive analysis of μ(N;T) in the case of an interacting gas in Popov approximation and beyond it. He found an essential relation which describes the condensate potential and non-condensate potential as:

$$\mu = n_c \mu_c + n_{nc} u_{nc} \quad (10)$$

Where $n_c = \frac{N_c}{N}$ and $n_{nc} = \frac{N_{nc}}{N}$ presents the condensate and non-condensate fraction respectively. μ_{cis} chemical potential relative to the condensate atoms and μ_{nc} is the non-condensate chemical potential. We used the algorithm described in ref [35] so at each iteration we determine total chemical potential by used equation (10), and consequently the condensate and non-condensate chemical potential. We plot in **FIG.1** the general variation of chemical potential for various temperature (up to the transition temperature T_c for N = 2000.We note that the tendencies of the both chemical potential are the same just up to 0:74Tc but when we go beyond it the total chemical potential stars to deviate which is the result of the dominance of the potential created by the non-condensate atoms.

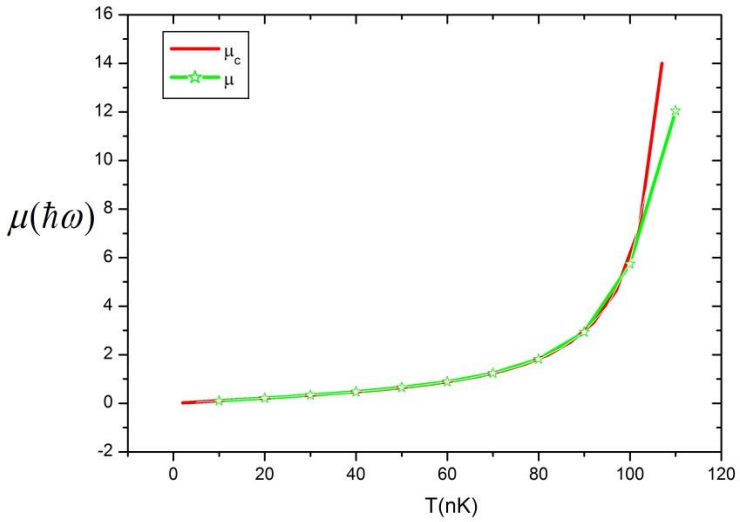

FIG. 1. The chemical potential versus temperature, the solid line corresponds to the condensate chemical potential; the solid line with stars (green) corresponds to the total chemical potential.

In order to examine in detail how the interactions affect, by changing the strength coupling g, this physical quantity we choose as example a Thomas Fermi limit. Recall that in this limit we neglect the kinetic part of equation (1), we find directly an analytic form of the condensate function φ_0 (r):

$$\left|\varphi TFT\,(r)\right|^2 = \frac{(\mu - V_{trap}(r))}{gN_c} - \frac{(2\tilde{n}(r) + \tilde{m}(r))}{N_c} \quad (11)$$

$$n_c TFT(r) = n_{cTF0}(r) - (2\tilde{n}(r) + \tilde{m}(r)) \quad (12)$$

Where $n_cTFT(r)$ and $n_{cTF0}(r)$ are the Thomas Fermi density at finite temperature T and at zero temperature respectively. The **FIG. 2** shows the general variation of the condensate density in Thomas Fermi approximation (TFA) and in (GHFB) approximation.

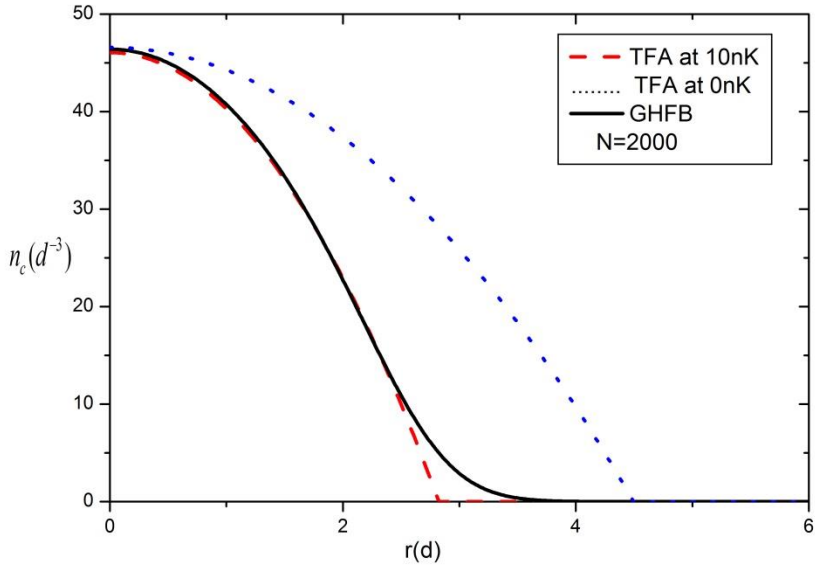

FIG. 2. The condensate density in (GHFB) as solid line, the dashed line Thomas Fermi approximation at T=10nK and the dotted line is the Thomas Fermi approximation at T=0nK.

The dashed lines correspond to the Thomas-Fermi approximation (TFA) at finite temperature; the continuous line is the calculation given by (GHFB) approximation and the dotted line is the Thomas-Fermi approximation (TFA) at zero temperature. If we analyze this **FIG. 2** with more attention we deducted that it corresponds to a translation at the radius of the condensate which can be verified by a theoretical relationship given below and as consequence the Thomas Fermi chemical potential, μ_{TFT} (T), and radius, R_{TFT} (T),at finite temperature can be obtained by using the following condition:

$$\int_0^{R_{TFT}} d^3r \left|\varphi_{TFT}(r)\right|^2 = 1 \qquad (13)$$

$$\mu_{TFT}(T) = \mu_{TF0}(0)(1+2\frac{\tilde{N}}{N_c}+\frac{\tilde{M}}{N_c})^{\frac{2}{5}} \qquad (14)$$

$$R_{TFT}(T) = R_{TF0}(0)(1+2\frac{\tilde{N}}{N_c}+\frac{\tilde{M}}{N_c})^{\frac{1}{5}} \qquad (15)$$

Where $\mu_{TF0}(0) = \frac{\hbar\omega}{2}(15\frac{N_{ca}}{d})^{\frac{2}{5}}$ is chemical potential at 0nK and $\int_0^r d^3r\tilde{n}(r) = \tilde{N}, \int_0^r d^3r\tilde{m}(r) = \tilde{M}$

We assume that at finite temperature the contribution of thermal cloud is small compared that the condensed atoms density where the following approximation $\frac{\tilde{N}}{N_C} << 1$ and $\frac{|\tilde{M}|}{N_C} << 1$ is satisfactory. The equations (11) and (12) can be reduced and finally the chemical potential μ_{TFT} (T) and radius R_{TFT} (T) take the new form:

$$\mu_{TFT}(T) \approx \mu_{TF0}(0)(1+\frac{4}{5}\frac{\tilde{N}}{N_C}+\frac{2}{5}\frac{\tilde{M}}{N_C}) \quad (16)$$

$$R_{TFT}(T) \approx R_{TF0}(0)(1+\frac{5}{5}\frac{\tilde{N}}{N_C}+\frac{1}{5}\frac{\tilde{M}}{N_C}) \quad (17)$$

By explaining this later term, we deducted that:

$$R_{TFT}(T) = R_{TF0}(0) - R_1(T) \quad (18)$$

Where R_1(T) is the translator vector.

In **FIG. 3** we plot the chemical potential μTFT (T) of interacting gas as a function of condensate number N_c and at the specific temperature 0:74Tc. We used the parameters g=1, g=2 and g=4 for various number of condensate (where $g' = \frac{4\pi\hbar a}{d}\hbar\omega g$. The solid line correspond to g=1, the dashed line correspond to g=2 and the dotted line correspond to g=4.

We note that when we increase g, the chemical potential, μ_{TFT} (T), decrease. Noted here that the specific temperature is determined by putting:

$$N_c = \tilde{N} \quad (19)$$

Where $\frac{N_C}{N} = (1-(\frac{T}{T_C})^{\alpha})$ with α=2.3 is fitting parameters.

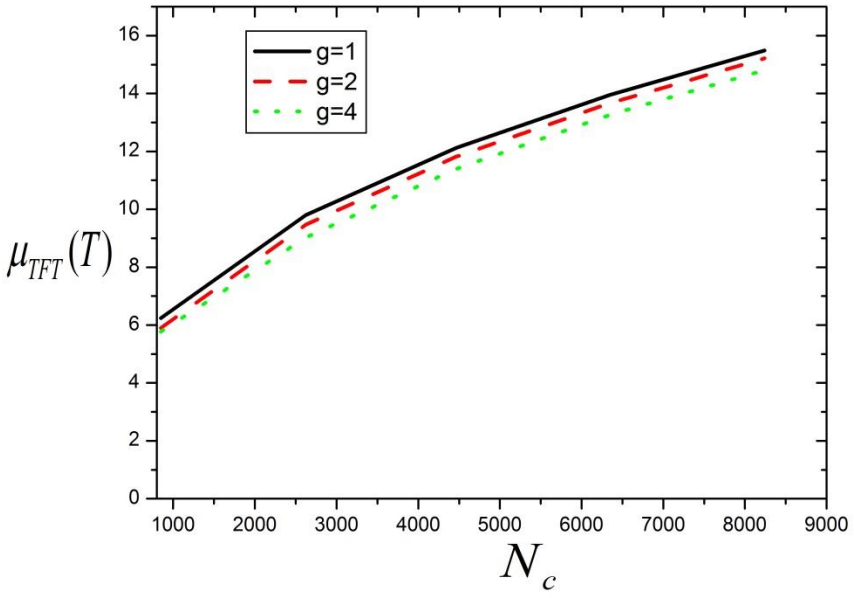

FIG. 3. The chemical potential in Thomas Fermi approximation at finite temperature T=0:74Tc for g=1, 2 and 4:the dashed line g=2, dotted line g=4, solid line g=1as functionas the condensate atoms number Nc.

Condensed, non-condensed and anomalous fraction

We use the equations (5), (6) and (7) and we integrated over all space, we can determine the condensed, non-condensed and anomalous fractions. We plotted these fractions as function of temperature with N=10000 for various strength coupling g=1 and g=2 in **FIG. 4**.The presence of the repulsive interactions has the effect of expanding the atomic cloud. We note here that the non-condensate fraction increases monotonically with the strength coupling g while the condensate fraction decrease with g. The anomalous fraction increases if we take the absolute value. Before finish, we present this fraction at just 0:74Tc as function of number of particles ranging from 2000 to 10000 for g. The **FIG. 5** shows their variations which present a monotonically comportment. The figure 5 shows their variations which present a monotonically comportment.

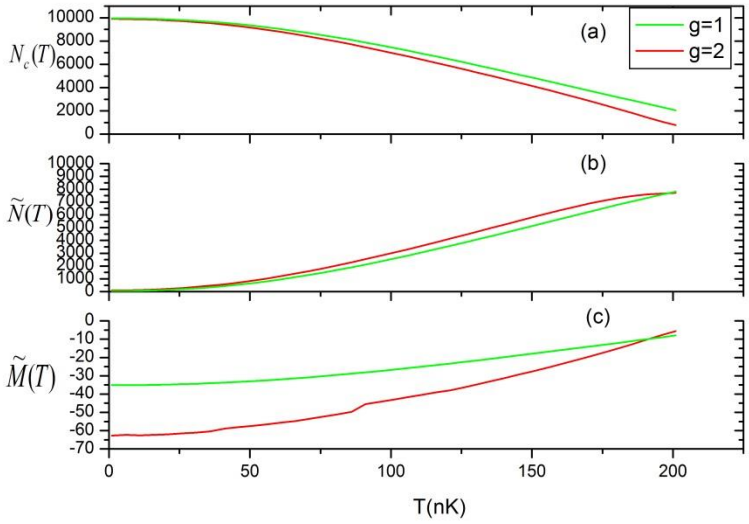

FIG. 4. (a) The condensate fraction, (b) non-condensate fraction and (c) anomalous fraction in the condition of [5]; N=10000 for g=1 and 2.

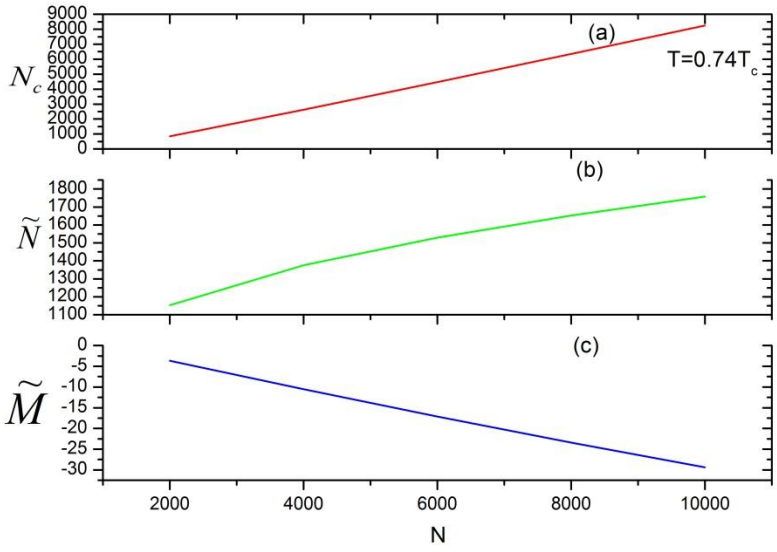

FIG. 5. (a) The condensate fraction, (b) non-condensate fraction and (c) anomalous fraction in the condition of [5] as function as the number of atoms at T = 0:74Tc with g=1.

Heat capacity

For a gas of particles in a constant confining potential, the most useful definition of the heat capacity is [36]:

$$C_n(T) = \frac{1}{2N}|T \qquad (20)$$

For our case the energy is given by:

$$E(T,N) \equiv \mu(T,N) \qquad (21)$$

In Thomas Fermi approximation (TFA) the equation (20) takes the new form:

$$C_{nTF}(T,N) = \frac{1}{2N}\mu_{TF0}(0)\frac{4}{5}\alpha\frac{T^{\alpha-1}}{T_c^{\alpha}} \qquad (22)$$

In **FIG. 6**, we plot the heat capacity in Thomas Fermi approximation as function as temperature for N=2000 and with different strength coupling g. We note that this capacity for N=2000 has a same behavior for different g until 40 nK and beyond this value it stars to decrease gradually when g increases. For more precision, we present it in **FIG. 7** as function as Nc at T fixed, we choose T=0:74 Tc, because at this specific temperature the effect of the potential created by the non-condensed atoms has the same that their created by the condensed atoms. We note that the effect of the interaction on the heat capacity depends on the strength of the interactions, g which decrease when we increase g, but when we exceeds a critical value Nc=4500 the three curves have the same behavior.

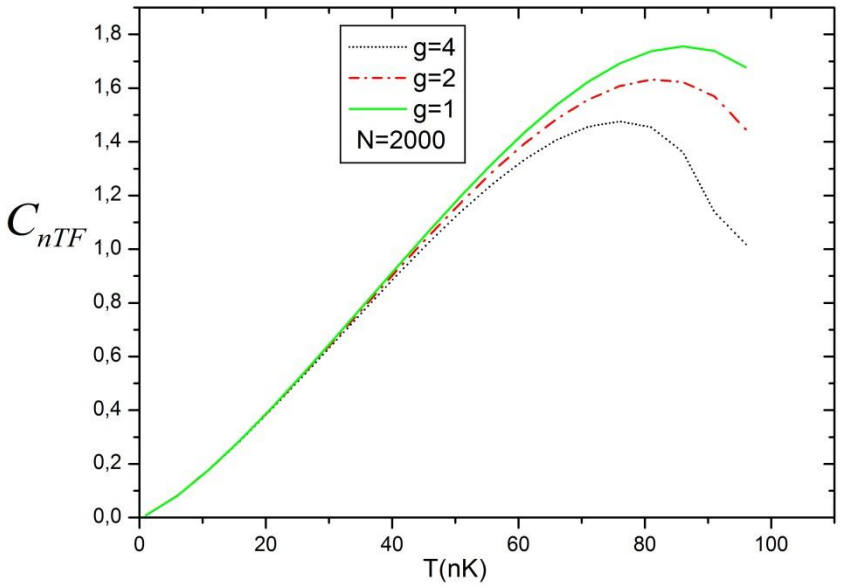

FIG. 6. The heat capacity in TF approximations versus the temperature of N=2000 for various strengths coupling g. The solid line correspond to g=1, the dashed line correspond to g=2 and the dotted line correspond to g=4.

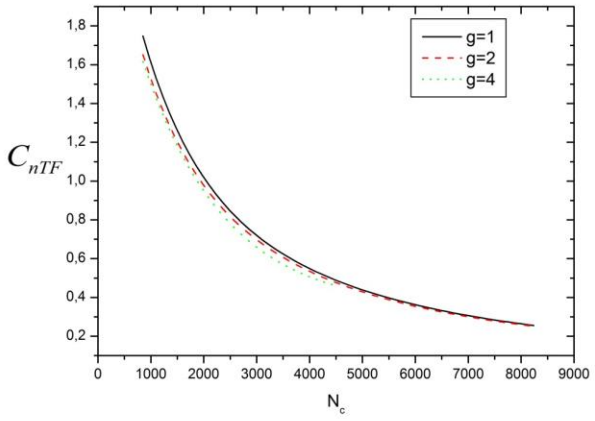

FIG. 7. The heat capacity in units of kB versus the condensate number for g=1, 2 and 4 at T=0:74 Tc : the dashed line g=2, the dotted line g=4 and the solid line g=1.

Collective excitation

The study of elementary excitations is important case of quantum many body theories in general and in particular for Rb gases. In this case, we have plotted the collective excitations as a function of number of atoms for various coupling strengths g=1 and g=2 at finite temperature T=0:74Tc, the effect of non-condensate atoms is not negligible as consequently the potential created by this fraction start to increase.

The **FIG. 8**, shown the frequencies modes. We observe that the frequency modes l=0 and l=2 splits into two parts which characterize the degenerate eigenvalue of the harmonic potential. The l=0 mode, also called Breathing mode, is influenced by the compressibility of the condensate, and its increase in frequency which is the result of repulsive interactions between atoms. On the other hand, the mode, l=2, or quadruple mode frequency decreases when we increase N and g respectively. The mode l=1 present the center of mass of the condensate mode and is located precisely at ω_{trap}. This later is not affected by the interaction effect.

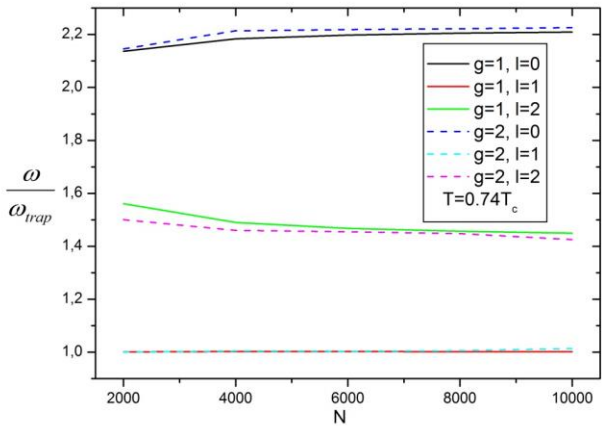

FIG. 8. The calculated excitation frequencies as function as the number of atoms N at T=0:74Tc for g=1 and g=2.

Aspect ratio

Another quantity which measures the mutual interactions between the condensate and the thermal cloud is the aspect ratio. At finite temperature it presents the ratio between the kinetic energy and the mean field energy created by the condensate atoms and the energy created by the thermal cloud and can be written as:

$$AR_{\tilde{n}} = \frac{T}{< gn_C(r) + 2g\tilde{n}(r) >} \quad (23)$$

With T is the kinetic energy. We assume that the thermal cloud effect is less than the condensate effect $\frac{n_C(r)}{\tilde{n}(r)} |<< 1$. The equation (23) takes a new form:

$$AR_{\tilde{n}} \approx AR_{w\tilde{n}}(1 - 2\frac{n_C(r)}{\tilde{n}(r)}) \quad (24)$$

Where $AR_{w\tilde{n}} = \frac{T}{<gn_C(r)>}$ is the aspect ratio without the thermal cloud.

The **FIG. 9** depicts this ratio (AR) at zero temperature, ARwen,and at finite temperature, AR_{en}, as function of the number of condensed atoms as predicted by GHFB calculations and measured by [37]. We observe that the GHFB approximation yields an overall good agreement with experiment and confirms the departure from the TF model [38-39] of Castin-Dum which predicts a constant aspect. The aspect ratio at finite temperature presents instability around 1.05.

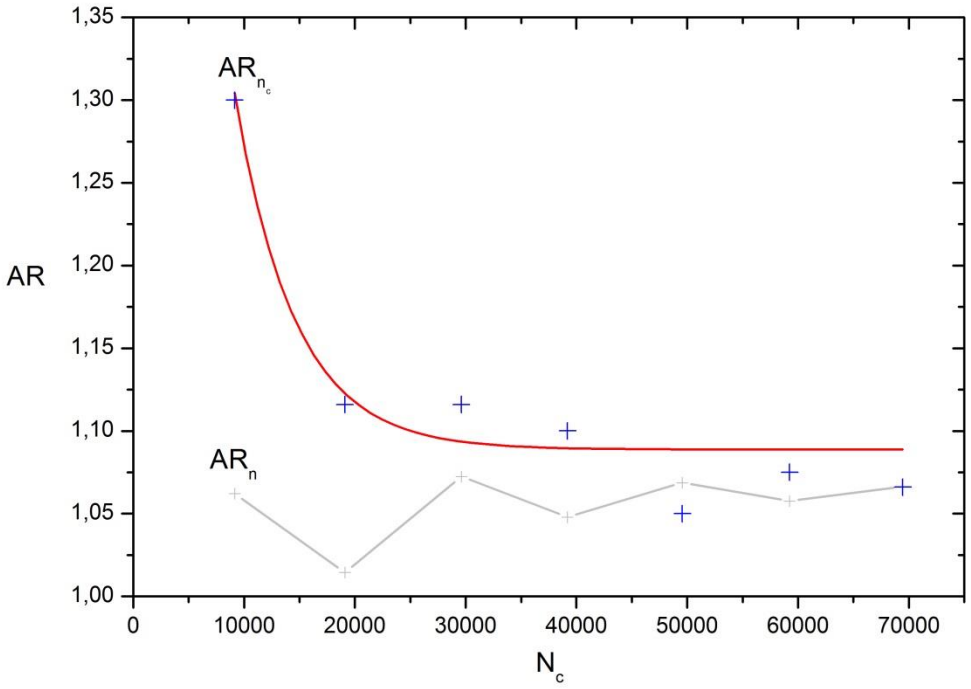

FIG. 9. Aspect ratio of pure BEC versus the condensate number Nc. Solid line represent the GHFB calculations while crosses (blue) are from [37].

Conclusion

We have concerned in this paper, a behavior GHFB equations of interacting Bose gases in a harmonic trap at finite temperature. So about this, we have developed a numerical code to solve the GHFB equations for large numbers of atoms, where the real numerical challenge is not the number of atoms but the number of occupied modes at finite temperature inspired by the anomalous density. As consequence, we have determined a chemical potential of the condensed atoms and a chemical potential of the non-condensed atoms. We have discussed their behavior and their effect when we change the coupling constant and particularly in Thomas Fermi limit at finite temperature. We find that the interactions have, above a specific temperature, an essential effect in structure of these different quantities appeared, the thermal cloud increase but the chemical potential and the condensate density decrease. The aspect ratio, at finite temperature, presents an instability value around 1.05 and conforms to the experimental data [37] at zero temperature.

Acknowledgments

I would like to thank N. Van Giai for his helpful comments on the numerical algorithm and for his warm hospitality at the Theoretical Division of the Nuclear Physics Institute Orsay France.

REFERENCES

1. MH Anderson, JR Ensher, MR Matthews, et al. Observation of Bose-Einstein Condensation in a Dilute Atomic Vapor, Science 1995;269: 198-201.
2. KB Davis, MO Mewes, M R Andrews, et al. Phys Rev Lett 1995;75: 3969.
3. CC Bradley, CA Sackett, JJTollett, et al. Phys Rev Lett 1997;79: 1170.
4. EA Cornell and CE Wieman. Rev Mod Phys. 2002;74: 875.
5. CC Bradley, CA Sackett, JJ Tollett, et al. Phys Rev Lett 1995;75: 1687.
6. DAW Hutchinson, K Burnett, RJ Dodd, et al. J Phys B: At Mol Opt Phys 2000;33: 3825-3846.
7. NP Proukakis, SA Morgan, S Choi, et al. Comparison of gapless mean-field theories for trapped Bose-Einstein condensates. Phys Rev A 1998;58: 2435.
8. AL Fetter. Ann Phys. 1972;70: 67.
9. NN Bogoliubov. On the Theory of Superuidity. J Phys 1947;11: 23.
10. LD Landau. J Phys 1941;5: 71.
11. EA Uehling, GE Uhlenbeck. Phys Rev 1933;43: 552.
12. O Penrose and L Onsager. Phys Rev. 1956;104: 576.
13. K Huang and CN Yang. Phys Rev. 1957;105: 767.
14. ST Beliaev. Sov Phys JETP 1958;7: 289.
15. ST Beliaev. Sov Phys JETP 1958;7: 299.
16. NM Hugenholtz and D Pines. Phys Rev. 1959;116: 489.
17. PC Martin and J Schwinger. Phys Rev 1959;115: 1342.
18. G Baym and LP Kadano. Phys Rev 1961;124: 287.

19. F Takano. Phys Rev. 1961;23: 699.

20. LP Kadano and G Baym. Quantum Statistical MechanicsNew York: Benjamin, 1962.

21. PC Martin. J Math Phys. 1963;4: 208.

22. J Gavoret and P Nozieres. Ann Phys. 1964;28: 349.

23. LV Zh Keldysh. Eksp Teor Fiz. 1964;47: 1515.

24. JW Kane and LP Kadano. J Math Phys. 1965;6: 1902.

25. PC Hohenberg and PC Martin. Ann Phys. 1965;34: 291.

26. VN Popov. Functional Integrals and Collective Excitations. Cambridge University Press. 1987.

27. ND Mermin and H Wagner. Phys Rev Lett. 1966;22: 1133.

28. PC Hohenberg. Phys Rev. 1967;158: 383.

29. SA Morgan. J Phys 2000;33: 3847.

30. PO Fedichev and GV Shlyapnikov. Phys Rev A 1998;58: 3146.

31. VN Popov and LD Fadeev. Soviet Physics JETP 1965;20: 890.

32. H Shi and A Grifin. Phys Reps. 1998;304: 1.

33. RJ Dodd, M Edwards, CW Clark, et al. Phys Rev A. 1998;57: 32.

34. VI. Yukalov. Laser Phys Lett. 2006;3: 40614.

35. S Kouidri and M Benarous. J Phys. 2011;44: 205301.

36. JR Ensher, DS Jin, MR Matthews, et al. Phys Rev Lett. 1997;77: 4984.

37. M Zawada, R Abdoul, J Chwedenczuk, at al. J Phys 2008;41: 241001.

38. Y Castin and R Dum. Phys Rev Lett. 1996;77: 5315.

39. W Ketterle, DS Durfee and DM Stamper-Kum Pro. Int. School of Physics Enrico Fermi, Course CXL. 67-176.